Tuned physical characteristics of PbSe binary compound: a DFT study

L. Shoukat[a], M. K. Butt[a], S. Saleem[a], Z. M. Elqahtani[b], S. A. Aldaghfag[b], M. Ishfaq[a], M. Yaseen[a,*] , E. Yousef[c,d], H. H. Hegazy[c, d]

[a]*Spin-Optoelectronics and Ferro-Thermoelectric (SOFT) Materials and Devices Laboratory, Department of Physics, University of Agriculture Faisalabad 38040, Pakistan*
[b]*Department of Physics, College of Sciences, Princess Nourah bint Abdulrahman University, P. O. Box 84428, Riyadh 11671, Saudi Arabia*
[c]*Research Center for Advanced Materials Science (RCAMS), King Khalid University, Abha 61413, P. O. Box 9004, Saudi Arabia.*
[d]*Physics Dep., Faculty of Science, King Khalid University, P. O. Box 9004, Abha, Saudi Arabia.*

Physical features of transition metal (TM) doped lead selenide, $Pb_{1-x}Cr_xSe$, $Pb_{1-x}Co_xSe$ and $Pb_{1-x}Ni_xSe$ (x=0% and 25%) have been investigated by ab-inito method. The exchange correlation energy is computed by generalized gradient approximation (GGA). A direct band gap (E_g) of 0.35 eV has been observed for PbSe. The analysis of spin-resolved electronic band structure (BS) and density of states (DOS) reveal the half-metallic ferromagnetic (HMF) character of doped compounds. In addition, the calculated magnetic moments (μB) of $Pb_{1-x}Cr_xSe$, $Pb_{1-x}Co_xSe$ and $Pb_{1-x}Ni_xSe$ compounds are found to arise due to doped transition metals and confirmed by 3D spin-polaized iso-surface density plots. The optical features including optical conductivity σ(ω), absorption coefficientα(ω), extinction coefficient k(ω), refractivity R(ω), dielectric function and refractive index n(ω) have been calculated to envisage the optical response of given materials. Further, the BoltzTrap code has been implemented to probe the thermoelectric characteristics in term of power factor (PF), Seebeck coefficient (S), thermal and electrical conductivity. The outcomes of calculations divulge that $Pb_{1-x}X_xSe$ (X=Cr, Co, Ni) would be suitable candidates for both optoelectronics and thermoelectric applications.

(Received May 29, 2022; Accepted September 6, 2022)

Keywords: Transition metals, Spintronics, Absorption, DFT

1. Introduction

In the current decades, HMF compounds gained attention due to their efficient performance in optoelectronic and spintronic devices. Such materials display 100% spin-polarization as one spin channel demonstrate metallic behavior (down/up) and other spin shows semiconducting character [1-3]. In 1983, half-metallic (FM) behavior was 1st detected during the study of half-Heusler compound (NiMnSb) by de Groot and his colleagues [4]. Later on, several other compounds displayed HM behavior upon doping with some sort of elements [5]. Lead chalcogenides semiconductors demonstrate unique optical and electronic properties [6]. PbSe also belongs to these chalcogens (IV-VI) and becomes a topic of interest due to its different transport and electronic characteristics such as small E_g, high carrier mobilities and dielectric constants, low resistivity and positive temperature coefficients [7-9]. These characteristics make them appropriate applicant for various advanced usages like infrared laser diodes, optoelectronic, thermo-electronic and spintronic devices and various detectors.

* Corresponding author: myaseen_taha@yahoo.com
https://doi.org/10.15251/JOR.2022.185.649

In recent years, large number of materials like as CrO_2[10], Fe_3O_4[11], Cs_2NaMCl_6 (M = Ti, V, Mn) [12], $NdInO_3$[13], $CeAlO_3$, $PrAlO_3$[14], Cr-doped CdTe[15], Cr-doped BeSe and BeTe[16], Mn-doped ZnS[17] with various structures and chemical composition have been reported to display HM nature. Chattopadhyaya et al., investigated the alternation in structural and optoelectronic behavior of Ba doped PbY (Y=S, Se and Te) using FP-LAPW approach. The electronic parameters display direct E_g for PbY (Y=S, Te and Se) compounds, which transform into indirect E_g after doping of Ba. The values of zero frequency limit of optical parameters such as $\varepsilon_1(0)$, R(0) and n(0) upsurges with the rise in atomic number of the doping element in the ternary alloys and binary compounds. However, a non-linear change was observed between the highest values of optical conductivity and concentration of the dopant [18]. Boukhris et al., investigated the physical properties of PbSe, BeTe and PbS compounds using LDA and GGA approaches and revealed the direct E_g. Furthermore, the thermal characteristics was estimated by implementing the quasi harmonic Debye model[6].

In this work, magnetic, optoelectronic and TE properties of $Pb_{1-x}Cr_xSe$, $Pb_{1-x}Co_xSe$ and $Pb_{1-x}Ni_xSe$ (x=0 and 25%) are theoretically studied. TMs are doped in the host PbSe to check the spin-polarized electronic BS. Literature survey divulges that there is no enough literature related to the effects of TM doping on physical characteristics of the PbSe.

2. Method of calculation

PbSe has rock-salt structure and crystallizes in cubic form (space-group Fm-3m)[19] with lattice constants 6.124 Å [20, 21]. The FP-LAPW [22] scheme is adopted for the computational study of magnetic and electronic of PbSe, $Pb_{1-x}Cr_xSe$, $Pb_{1-x}Co_xSe$ and $Pb_{1-x}Ni_xSe$ (x=25%). In this scheme, the space is partitioned into two portions: interstitial and muffin-tin spheres. In interstitial part, the basis sets are comprised of plane waves; however, in muffin-tin part, the basis set is explained by radial solution of one particle Schrodinger equation. Inside the sphere, the valence wave function is expended upto l_{max}=10. Inside the interstitial part, the plan wave is expended with cut off of $R_{MT}*K_{MAX}$ = 7, where K_{MAX} and R_{MT} are highest value of reciprocal vector and muffin-tin radius, respectively. All calculations are performed with a mesh of 1000-k points in the irreducible Brillouin zone. Moreover, to avoid the leakage of energy cut-off energy was set at -6.0 R_y. Pb is positioned at 4a (0, 0, 0) and Se atoms at 4b (1/2, 1/2, 1/2) in the cell. The states of Pb ($5d^1$ $6s^2$ $6p^2$), Se ($3d^{10}$ $4s^2$ $4p^4$), Cr ($3d^5$ $4s^1$), Co ($3d^7 4s^2$) and Ni ($3d^8 4s^2$) are taken as valence electrons. The RMT values are selected as 2.05, 1.75 and 2,5 bohr for Pb, Se, and for doping atoms (Cr, Co and Ni), correspondingly.

3. Results and discussions

3.1. Band structures

The electronic BS of PbSe, $Pb_{1-x}Co_xSe$, $Pb_{1-x}Cr_xSe$ and $Pb_{1-x}Ni_xSe$ (x= 25%) are calculated using PBE-GGA approximation. The outcomes demonstrate the direct-gap semiconducting character of PbSe at the L-L points (see Fig. 1). The spin-resolved BS of Cr-doped PbSe illustrate the metallic BS in spin up and semiconductor in down state (see Fig. 3). However, the BS of Co and Ni doped PbSe display semiconductor behavior in spin up and metallic features on the other spin (see Fig. 2 and 4). The measurement of HM gap is calculated from the VBM and E_F. This illustrate the least amount of energy is required to shift an electron from the VB to the E_F [23]. The computed value of E_g for PbSe is 0.34 eV, which is in accordance to the reported data [24]. In addition, the HM E_g for $Pb_{1-x}Co_xSe$, $Pb_{1-x}Ni_xSe$ and $Pb_{1-x}Cr_xSe$ are 0.57, 0.48 eV and 0.34 eV, correspondingly. It is observed that the values of E_g declines from Co to Cu [25].

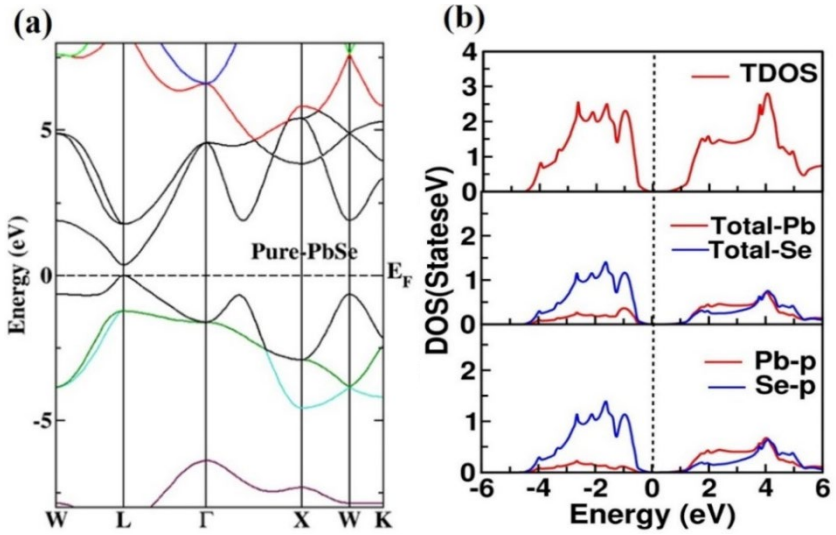

Fig. 1. (a) BS and (b) DOS of PbSe

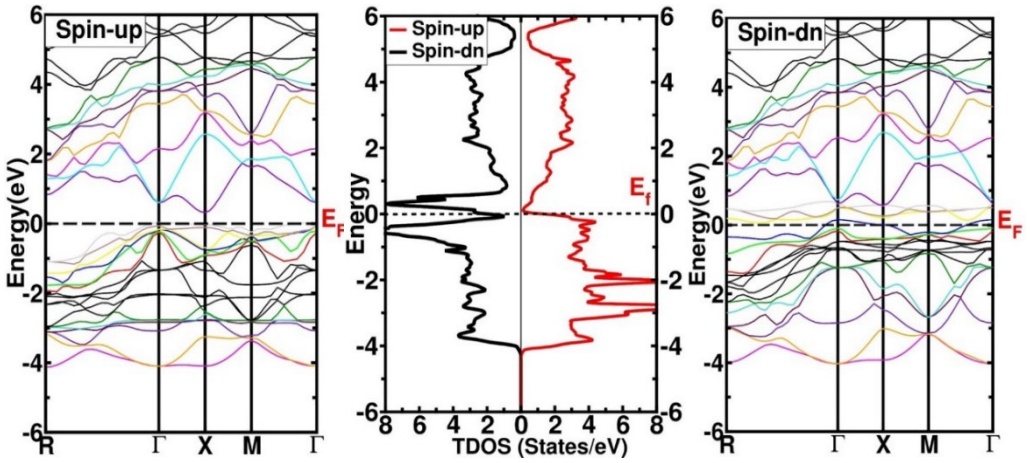

Fig. 2. BS of $Pb_{1-x}Co_xSe$ at x= 25%.

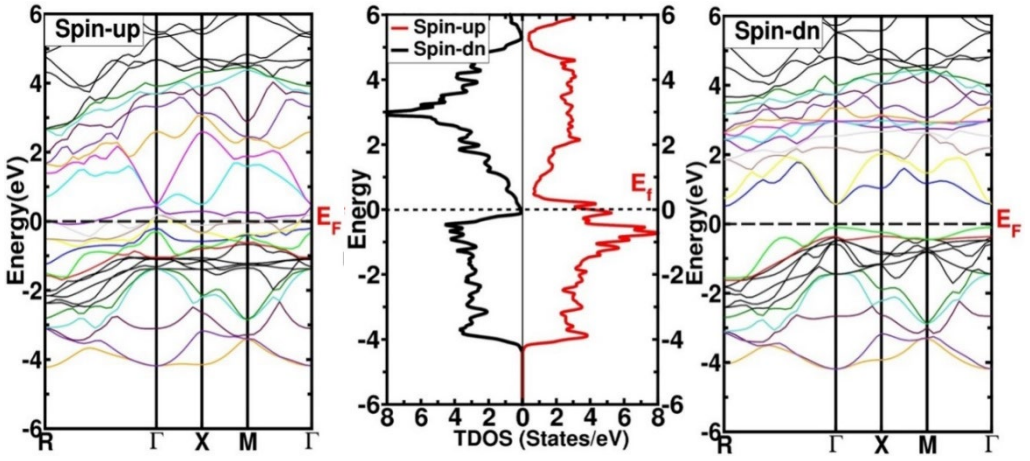

Fig. 3. BS of $Pb_{1-x}Cr_xSe$ at x= 25%.

DOS is associated with the energy distribution of states in the materials. For PbSe, PDOS is mainly dominated by Pb-*p* and Se-*p* states. For $Pb_{1-x}Cr_xSe$, the top of VB extended from -4 eV

to E_F, which is largely occupied by Cr-*d* hybridized with Se-*p* in majority spin and Se-*p* in minority spin (see Fig. 5). The sharp peak of Cr-*d* states has been observed at -1.9 (majority spin) and 3 eV (minority spin). The conduction band (CB) is majorly composed of Cr(*d)* with minute involvement of Pb(*p)*. For $Pb_{1-x}Co_xSe$ and $Pb_{1-x}Ni_xSe$, the dispersal of valence states exposes that the Co/Ni *d*-states are involved for the HM features of the discussed material. The occupancy of Co/Ni *d*-states at various locations in both states configuration indicate that electrons present in the states do not vanish out μB and leads to the ferromagnetic nature. In CB, the peaks of *d*-Co/Ni dominate in contribution with Pb-*p* states.

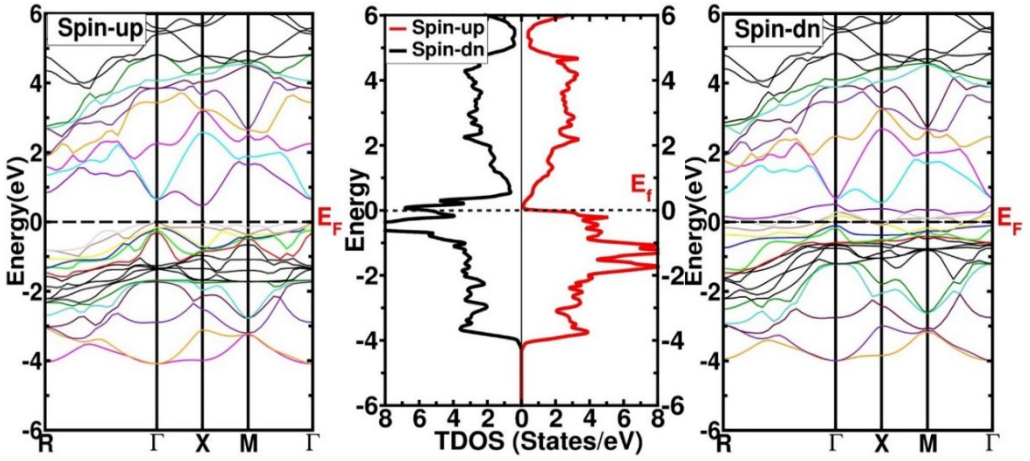

Fig. 4. BS of $Pb_{1-x}Ni_xSe$ at x= 25%.

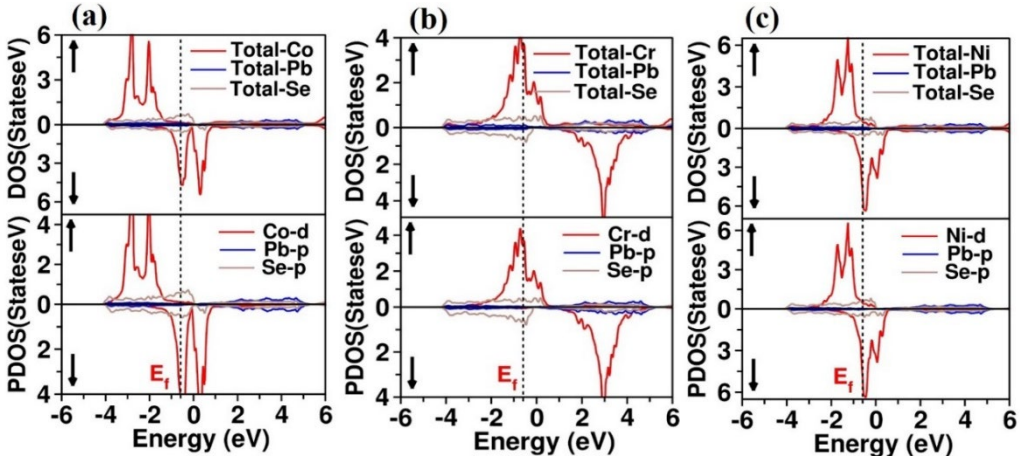

Fig. 5. PDOS of (a) $Pb_{1-x}Co_xSe$ (b) $Pb_{1-x}Ni_xSe$ (c) $Pb_{1-x}Ni_xSe$ at x= 25%.

3.2. Optical features

The optical properties are determined from the $\varepsilon(\omega)=\varepsilon_1(\omega)+i\varepsilon_2(\omega)$ (dielectric function) [30]. The doping of TMs increases the photon transition rate that creates free carriers in the CB. These carriers regulate the forward current [26]. Kramer–Kronig relation is adopted to determine the $\varepsilon_1(\omega)$ from $\varepsilon_2(\omega)$ [27]. The optical features are calculated by using following equations [28].

$$I(\omega) = \frac{4\pi}{\lambda}\left(\frac{[\varepsilon_1^2(\omega)+\varepsilon_2^2(\omega)]^{1/2}+\varepsilon_1(\omega)}{2}\right)^{1/2} \quad (1)$$

$$\sigma(\omega) = \frac{\omega}{4\pi}\varepsilon_2(\omega) \quad (2)$$

$$n(\omega) = \left(\frac{[\varepsilon_1^2(\omega)+\varepsilon_2^2(\omega)]^{1/2}+\varepsilon_1(\omega)}{2}\right)^{1/2} (3)$$

$$k(\omega) = \frac{\alpha\lambda}{4\pi} (4)$$

$$R(\omega) = \frac{[n(\omega)-1]^2+k^2(\omega)}{[n(\omega)+1]^2+k^2(\omega)} \quad (5)$$

$$\varepsilon_2(\omega) = \frac{Ve^2}{2\pi\hbar m^2\omega^2}\int d^3k \Sigma_{nn'} |< kn|p|kn' >|^2 f(kn) \times (1 - f(kn'))\delta(E_{kn} - E_{kn'} - \hbar\omega)) (6)$$

The dispersive part ϵ_1 (ω) and absorptive part ϵ_2 (ω) (see Fig. 6 (a, b)) of the undoped and doped PbSe are also explained. ϵ_1 (0) is a significant part that describes the electronic polarizability and fulfills the relation $n(0) = \sqrt{\epsilon_1}(0)$. From Fig. 6 (a), it can be seen that ϵ_1 (0) is increasing with different doping. Its values are 20.3, 51.6, 78.2, 115.4 for pure, Co, Cr and Ni doping, respectively. It demonstrates the highest peaks at (see Fig. 6 (a)) 1.1, 1.4, 1.5 and 2.4 eV for $Pb_{1-x}Ni_xSe$, $Pb_{1-x}Cr_xSe$, $Pb_{1-x}Co_xSe$ and PbSe, correspondingly. The negative value of $\varepsilon_1(\omega)$ shows the total reflectivity of incident electromagnetic (EM) wave from material, which corresponds to its metallic nature. The observed metallic effect may be due to the mismatch of E_g with falling electromagnetic wave and causes a complete reflection because only those radiation are absorbed which have large or equal energy than E_g [29]. The value of static dielectric constant $\varepsilon_1(0)$ is highest for $Pb_{1-x}Ni_xSe$ and lowest for PbSe. Moreover, $\varepsilon_2(\omega)$ has an incredible role in the assortment of optical material for optoelectronic device production. The $\varepsilon_2(\omega)$ illustrate the regions of EM spectrums in which the intensities of absorption of EM radiations are highest. The values of imaginary part are increased after doping with TM. The peak values of $\varepsilon_2(\omega)$ are obtained at 0.5, 0.4, 0.7 and 2.8 eV for $Pb_{1-x}Ni_xSe$, $Pb_{1-x}Cr_xSe$, $Pb_{1-x}Co_xSe$ and PbSe, respectively. After achieving peak intensities (see Fig. 6 (b)), $\varepsilon_2(\omega)$ start minimizing gradually.

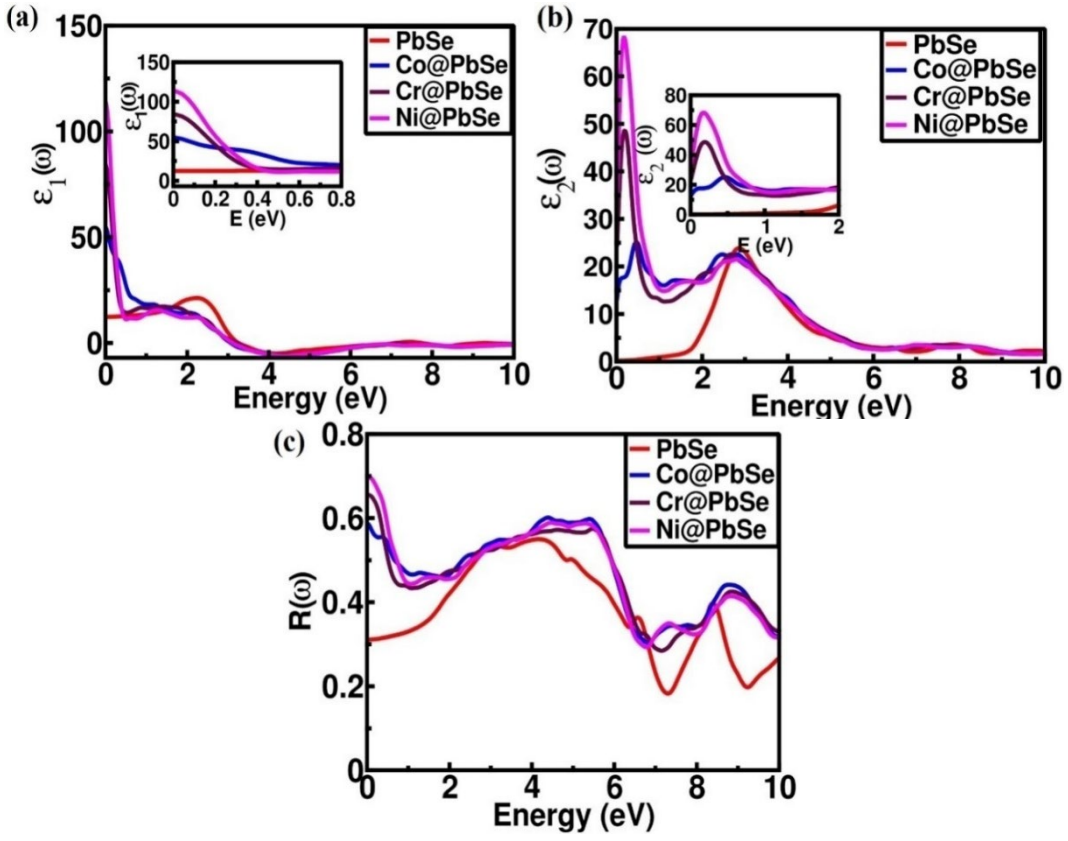

Fig. 6. (a) ε_1 (ω) (b) ε_2(ω) and (c) R (ω) for PbSe, $Pb_{1-x}Co_xSe$, $Pb_{1-x}Cr_xSe$ and $Pb_{1-x}Ni_xSe$ compounds.

The zero frequency R(0) is 0.31, 0.59, 0.63 and 0.66 for PbSe, $Pb_{1-x}Co_xSe$, $Pb_{1-x}Cr_xSe$, $Pb_{1-x}Ni_xSe$, respectively (see Fig. 6 (c)) and their maximum values in percentage are 70%, 65%, 59% and 50% at 4.91, 4.82, 4.76 and 4.61 eV, respectively. For these doping, the peaks in R(ω) curves are interrelated to peaks in dielectric functions, R(ω) value is highest in the regions where absorption is lowest.

The understanding of n(ω) is an essential feature to determine the application of optical compounds for photonic and optical devices. The values of n(ω) of Cr, Co and Ni doped PbSe compound is plotted against photon energy of upto 10 eV. The n(ω) and dielectric constant are interlinked with a relation $n(0) = \sqrt{\varepsilon(\omega)}$[30]. At zero frequency, the values of the n(ω) are 0.32, 0.59, 0.63 and 0.66 for PbSe, $Pb_{1-x}Co_xSe$, $Pb_{1-x}Cr_xSe$ and $Pb_{1-x}Ni_xSe$, respectively. The n(ω) follow a decreasing trend from 0 to 5 eV but after 5 eV the n(ω) become constant. For highly transparent materials, the n(ω) become nearly zero, however, the positive values of n(ω) correspond to highly absorptive materials. The n(ω) attained maximum values in the span of 2 to 3 eV for all mentioned materials (see Fig. 7 (a)). The k(ω) is calculated to estimate the absorption of light. The low value of k(ω) indicates that waves are passed through the material, while the positive values relates to the considerable absorption. The highest peaks are obtained in the visible region (see Fig. 7 (b)) indicating the usage of these materials in optical devices. The intensity of peak for $Pb_{1-x}Ni_xSe$ is high as compare to other compounds [26].The sharp absorption peaks are obtained at 8.2, 8.58, 8.6, and 4.38 eV for pure PbSe, $Pb_{1-x}Co_xSe$, $Pb_{1-x}Cr_xSe$ and $Pb_{1-x}Ni_xSe$, respectively (Fig. 7 c). After reaching maximum peak values it starts decreasing. The σ(ω) is another parameter depending on the interband and intraband transitions [31]. PbSe showed highest σ(ω) (9350.86 $\Omega^{-1}cm^{-1}$) at 2.95 eV. After doping of transition metals the value of σ(ω) is declined. The obtained σ(ω) values are 8678.57$\Omega^{-1}cm^{-1}$ for $Pb_{1-x}Co_xSe$, 8357.14 $\Omega^{-1}cm^{-1}$ for $Pb_{1-x}Cr_xSe$ and 8357.14 $\Omega^{-1}cm^{-1}$ for $Pb_{1-x}Ni_xSe$ at 2.88, 3.18 and 3.08 eV, respectively (see Fig. 7 (d)).

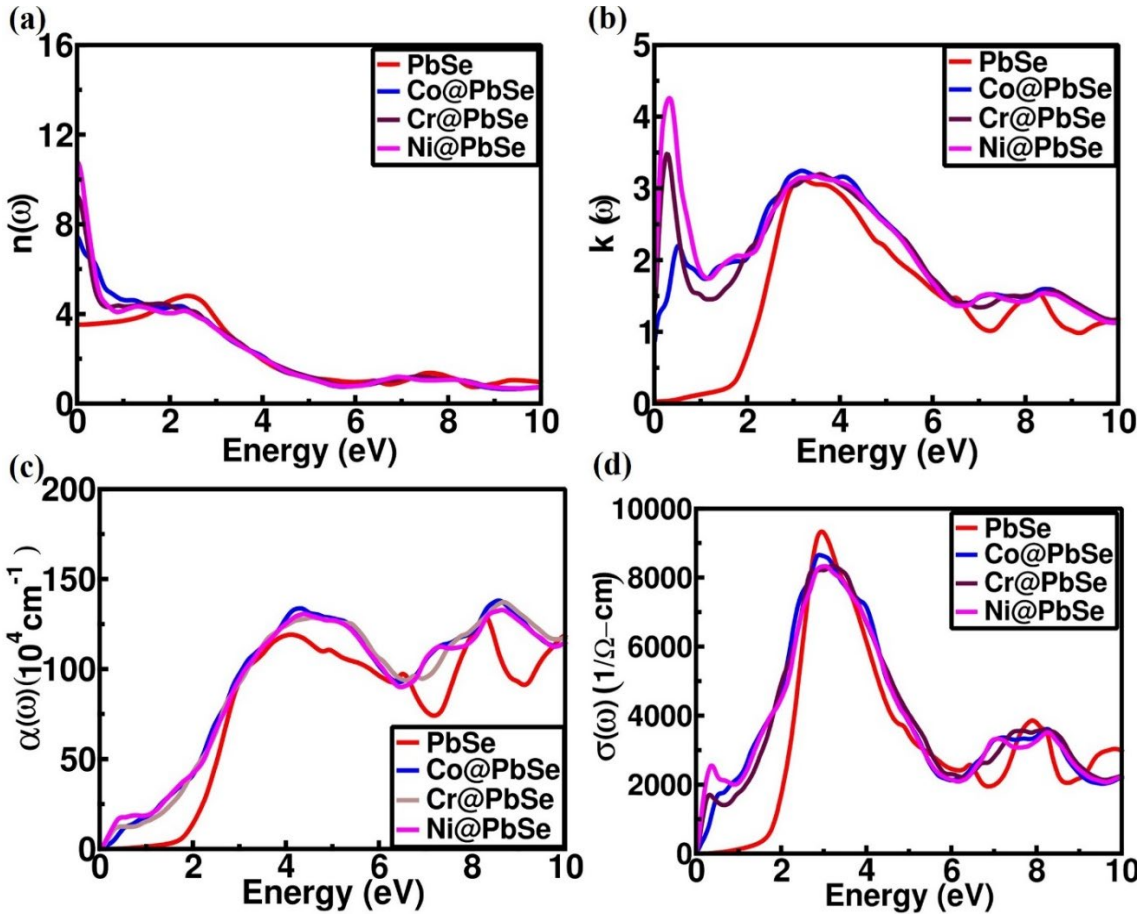

Fig. 7. (a) n (ω),(b) k (ω), (c) α (ω) and σ (ω) for PbSe, $Pb_{1-x}Co_xSe$, $Pb_{1-x}Cr_xSe$ and $Pb_{1-x}Ni_xSe$ compounds.

3.3. Thermoelectric properties

Due to the demand of energy, it is important to focus on sustainable energy sources and the energy produced from TE materials is an efficient as compare to various other types of energy sources such as fuel [32]. TE materials are utilized to produce power from the thermal energy emitted by the industry. These materials are useful for power generation and refrigeration [33], which proves the TE materials have various applications in energy gadgets [34, 35].

Ideal TE compounds posses large values of σ , S, PF and low k [36, 37]. The BoltzTrap package is used to elucidate figure of merit (ZT) σ, S, k_e, and PF for TM= Co, Cr and Ni doped PbSe (x=25%). σ express the flow of charge carriers and its increasing values with temperature represents the semiconductor behavior. The values of σ for Co, Cr, Ni doped and pure PbSe are 3.89×10^{19}, 6.21×10^{19}, 7.93×10^{19}, and 21.3×10^{19} $(\Omega\ m)^{-1}$, respectively at 200 K (see Fig. 8 (a)). It is found that pure PbSe has high σ than that of doped compound owing to the smaller E_g of PbSe that requires less energy to move electrons from VB to CB. k is consist of lattice (k_l) and electronic (k_e) parts, which is important to be optimized for the usage in TE gadgets because it conducts heat[38]. From the plot of k_e (see Fig. 8 (b)), it can be seen that the k_e for all doped and pure compounds increases from 3.664 to11.334 W/Kms, correspondingly (at 300 K) and then upsurge in a linear pattern to highest values at 800 K. The excellent TE material has high σ and low k_e [39]. S found the efficiency of thermocouples and can be calculated from S= ΔV / ΔT. The computed values S upsurges with temperature upto 800 K for pure and doped compounds (see Fig. 8 (c)). Its value is greater for Co@ PbSe than other at room temperature. The multiplication of S and σ is named as PF which is suitable for TE device performance [40] (see Fig. 8 (d)). The value of PF increases with the elevation of temperature for pure and doped compounds. Minimum PF values for pure and Cr/Ni doped PbSe occurred at 200 K. The computed PF for Co@PbSe reveals that it gains highest value at 530 K and almost remains constant up to 800 K.

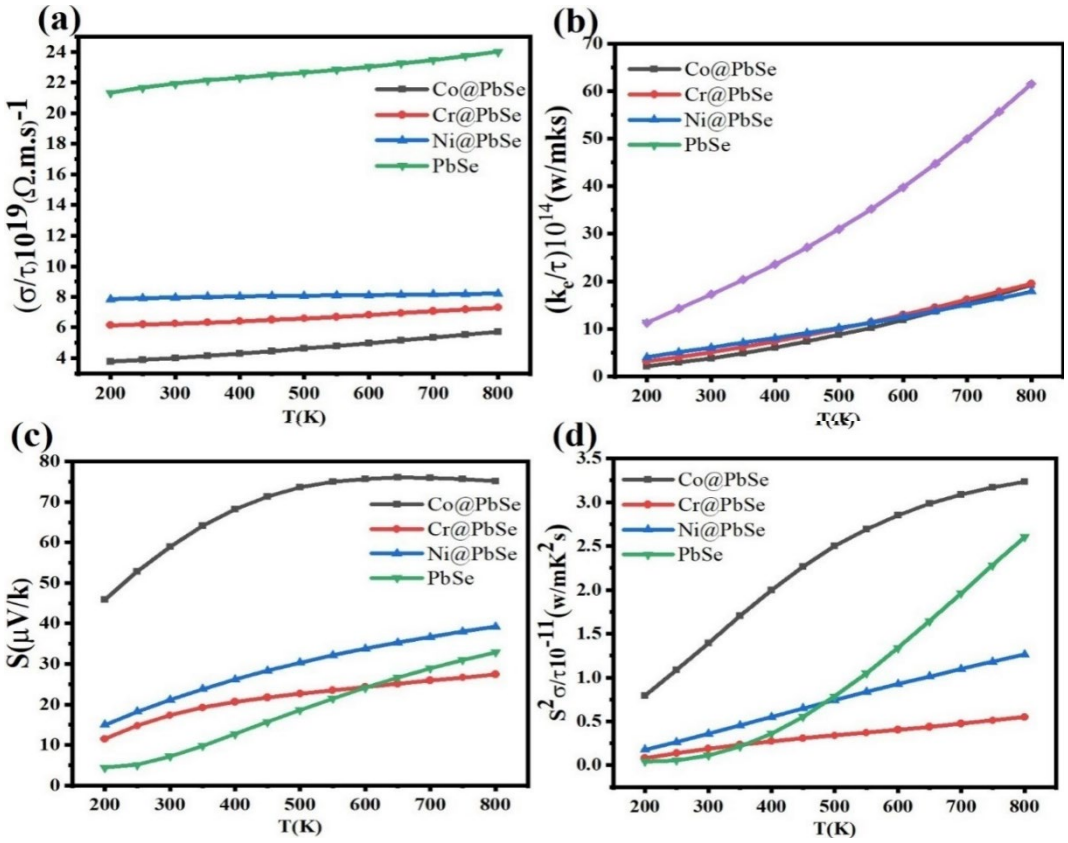

Fig.8. (a) σ *(b)* k *(c) S (d) PF for PbSe, $Pb_{1-x}Co_xSe$, $Pb_{1-x}Cr_xSe$ and $Pb_{1-x}Ni_xSe$ compounds.*

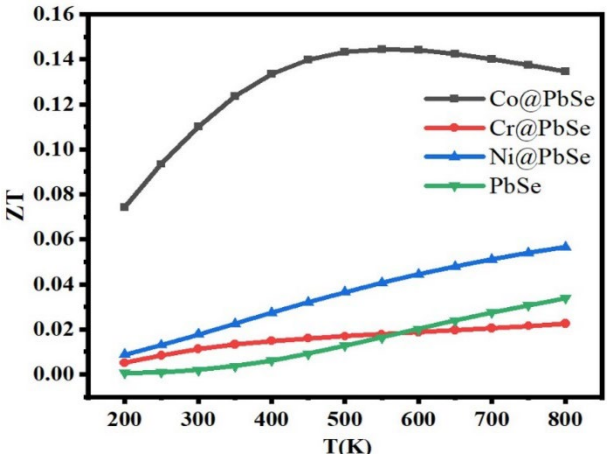

Fig.9. Plots of ZT.

In TE applications, the potential of materials is not only determined by PF-values but more accurately from ZT values.

$$ZT = \frac{S^2 \sigma T}{k} \quad (7)$$

The calculated ZT plots of studied compounds are exposed in Fig. 9. For Co@ PbSe, at low temperature (200 K), ZT is 0.078 and at high temperature (500 K), ZT is 0.145. Thus Co@PbSe has high S and ZT, suggests that it has promising thermoelectric applications.

3.4. Magnetic properties

PbSe is a non-metallic compound which becomes HMF after doping with Cr, Co and Ni.The total μB values are 4.00887, 2.95003 and 1.96770 μB for $Pb_{1-x}Cr_xSe$, $Pb_{1-x}Co_xSe$ and $Pb_{1-x}Ni_xSe$, respectively. The *d* states (unpaired electrons) of Cr, Co and Ni are responsible for the magnetization. The partial μB of Cr, Co and Ni are 3.98399, 2.3258, 1.09653 μ_B, respectively. Table 1 demonstrates the values of μB of given materials. Moreover, for the clarification of partial magnetic moment 3-dimensional iso-surface plots were plotted (see Fig. 10). It is observed that strong magnetization appears around the transition metals of Cr, Ni and Co. Also, the magnetization appears around the Se in all three doping elements because of the charge transfer due to different valences [41] and almost no magnetism was observed around the Pb elements.

Table 1. Magnetic moments of Ni, Cr and Co doped PbSe.

Magnetic moment	$Pb_{1-x}Cr_xSe$	$Pb_{1-x}Co_xSe$	$Pb_{1-x}Ni_xSe$
M_{int}	0.45581	0.12802	0.12122
M_{Cr}	3.98399	--	--_
M_{Co}	--	2.32583	--
M_{Ni}	--	--	1.09653
M_{Pb}	0.04068	-0.02179	-0.00997
M_{Se}	-0.13321	0.12298	0.18995
M_{total}	4.00887	2.95003	1.96770

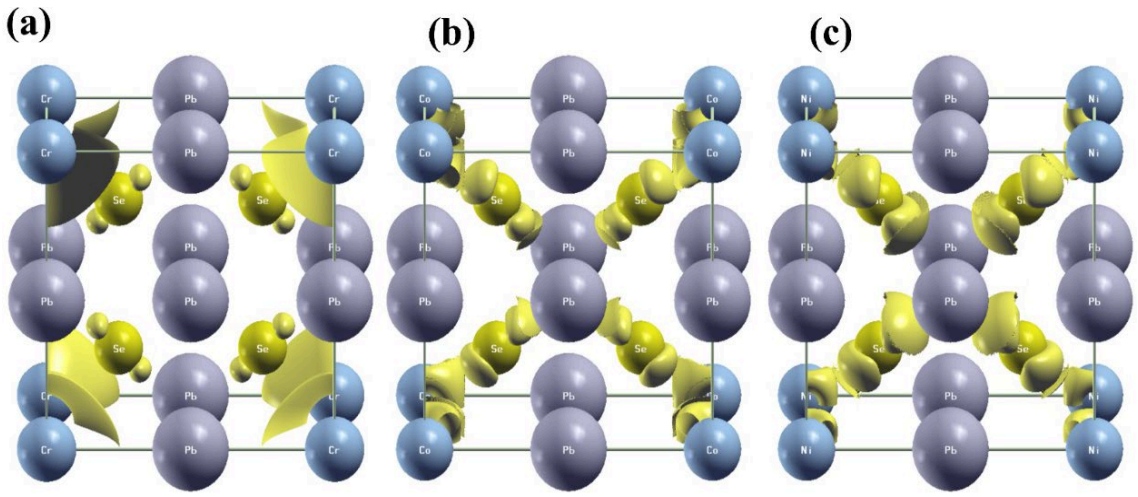

Fig. 10. Computed magnetic iso-surface plots of (a) $Pb_{1-x}Cr_xSe$ (b) $Pb_{1-x}Co_xSe$ and (c) $Pb_{1-x}Ni_xSe$ at x= 25%.

4. Conclusions

Here, the electronic, optical, thermoelectric and magnetic properties of PbSe, $Pb_{1-x}Co_xSe$, $Pb_{1-x}Cr_xSe$ and $Pb_{1-x}Ni_xSe$ (x=0% and 25%) using FP-LAPW scheme. Pure PbSe exhibits direct-gap semiconducting nature with E_g of 0.35 eV. The spin polarized electronic profile of $Pb_{1-x}Co_xSe$, $Pb_{1-x}Cr_xSe$ and $Pb_{1-x}Ni_xSe$ depicts the 100% spin polarization at the F_E and represents the HMF characteristics. The calculated magnetic moments are 4, 2.95 and 1.96 μB for $Pb_{1-x}Co_xSe$, $Pb_{1-x}Cr_xSe$ and $Pb_{1-x}Ni_xSe$, respectively, for further clarification spin-polarized iso-surface plots were studied to investigate the atomic contribution in magnetism. The *d* states mainly take part in magnetic behavior. The computed values of S and ZT for Co@PbSe are high, which shows that it is more promising material for TE applications. The outcomes reflect a significant achievement of TM doped PbSe for potential applications in spintronics, photoelectronic and TE gadgets.

Acknowledgements

This work was the support of King Khalid University, the Ministry of Education, and the Kingdom of Saudi Arabia for this research through a grant (RCAMS/KKU/004/21) under the research center for advanced material science. The authors also express their gratitude to Princess Nourah bint Abdulrahman University Researchers Supporting Project number (PNURSP2022R124), Princess Nourah bint Abdulrahman University, Riyadh, Saudi Arabia.

References

[1] J. De Boeck, Willem Van Roy, J. Das, V. Motsnyi, Z. Liu, L. Lagae, H. Boeve, K. Dessein, and G. Borghs, Semiconductor Science and technology 17(4), 342 (2002); https://doi.org/10.1088/0268-1242/17/4/307

[2] S.D. Sarma, American Scientist 89(6), 516-523 (2001); https://doi.org/10.1511/2001.6.516

[3] P. Sharma, Science 307(5709), 531-533 (2005); https://doi.org/10.1126/science.1099388

[4] R. A. De Groot, F. M. Mueller, P. G. Van Engen, and K. H. J. Buschow, Physical Review Letters 50(25), 2024 (1983); https://doi.org/10.1103/PhysRevLett.50.2024

[5] H.H. Xie, R.Y. Ma, Q. Gao, L. Li, and J.B. Deng, Chemical Physics Letters 661, 89-93 (2016); https://doi.org/10.1016/j.cplett.2016.08.063

[6] N. Boukhris, H. Meradji, S. A. Korba, S. Drablia, S. Ghemid, and F. el Haj Hassan, Bulletin of Materials Science 37(5), 1159-1166 (2014); https://doi.org/10.1007/s12034-014-0057-7

[7] R. A.Cowley, Philosophical Magazine 11(112), 673-706 (1965); https://doi.org/10.1080/14786436508230077

[8] I. V. Slipukhina, and D. M. Bercha, physica status solidi (b) 244(2), 650-668 (2007); https://doi.org/10.1002/pssb.200642263

[9] K. Murase, Ferroelectrics 35(1), 67-72 (1981);https://doi.org/10.1080/00150198108017666

[10] K. Schwarz, Journal of Physics F: Metal Physics 16(9), L211 (1986); https://doi.org/10.1088/0305-4608/16/9/002

[11] Q. Mahmood, B. U. Haq, M. Rashid, N. A. Noor, S. AlFaify, and A. Laref, Journal of Solid State Chemistry 286, 121279 (2020); https://doi.org/10.1016/j.jssc.2020.121279

[12] S. A. Mir, and D. C. Gupta, Journal of Alloys and Compounds 854, 156000 (2021); https://doi.org/10.1016/j.jallcom.2020.156000

[13] M. K. Butt, M. Yaseen, A. Ghaffar, and M. Zahid, Arabian Journal for Science and Engineering 45(6), 4967-4974 (2020); https://doi.org/10.1007/s13369-020-04576-6

[14] M. K. Butt, M. Yaseen, J. Iqbal, S. A. Abeer, A. Murtaza, M. Iqbal, and A. Laref. Journal of Physics and Chemistry of Solids 154, 110084 (2021);https://doi.org/10.1016/j.jpcs.2021.110084

[15] M. Yaseen, H. Ambreen, U. Shoukat, M. K. Butt, S. Noreen, S. Rehman, and S. M. Ramay, Journal of Ovonic Research 15(6), 401-409 (2019);

[16] S. M. Alay-e-Abbas, K. M. Wong, N. A. Noor, A. Shaukat, and Y. Lei, Solid State Sciences 14(10), 1525-1535 (2012); https://doi.org/10.1016/j.solidstatesciences.2012.08.020

[17] M. Yaseen, H. Ambreen, A. Sufyan, M. K. Butt, S. UrRehman, J. Iqbal, Misbah, S. Bibi, A. Murtaza, and S. M. Ramay, Ferroelectrics 557(1), 112-122 (2020)

[18] S. Chattopadhyaya, and R. Bhattacharjee, Journal of alloys and compounds, 694, 1348-1364 (2017); https://doi.org/10.1016/j.jallcom.2016.10.096

[19] S. V. Streltsov, A. Y. Manakov, A. P. Vokhmyanin, S. V. Ovsyannikov, and V. V. Shchennikov, Journal of Physics: Condensed Matter 21(38), 385501 (2009); https://doi.org/10.1088/0953-8984/21/38/385501

[20] M. Rashid, Z. Abbas, M. Yaseen, Q. Afzal, A. Mahmood, S.M. Ramay, Journal of Superconductivity and Novel Magnetism, 30(11), 3129-3136 (2017) https://doi.org/10.1007/s10948-017-4099-0

[21] S. Saleem, M.Yaseen, S. A. Aldaghfag, Misbah, R. Neffati, Phys. Scr. 97 095817 (2022) https://doi.org/10.1088/1402-4896/ac8a27.

[22] O. K. Andersen, Physical Review B 12(8), 3060 (1975);https://doi.org/10.1103/PhysRevB.12.3060

[23] B. Cai, X. Chen, M. Xie, S. Zhang, X. Liu, J. Yang, W. Zhou, S. Guo, and H. Zeng. Materials Horizons 5(5), 961-968 (2018); https://doi.org/10.1039/C8MH00590G

[24] K. K. Zhuravlev, Physica B: Condensed Matter 394(1), 1-7 (2007);https://doi.org/10.1016/j.physb.2007.01.030

[25] A. Anjami, A. Boochani, S. M. Elahi, and H. Akbari. Results in physics 7, 3522-3529 (2017); https://doi.org/10.1016/j.rinp.2017.09.008

[26] L. Pan, X. Liu, Z. Sun, and C. Q. Sun. Journal of materials chemistry A 1(29), 8299-8326 (2013); https://doi.org/10.1039/c3ta10981j

[27] A. B. Kuzmenko, Review of scientific instruments 76(8), 083108 (2005); https://doi.org/10.1063/1.1979470

[28] T. Tsafack, E. Piccinini, B. S. Lee, E. Pop, and M. Rudan. Journal of Applied Physics 110(6), 063716 (2011); https://doi.org/10.1063/1.3639279

[29] Mahmood, Q., M. Hassan, and M. A. Faridi, Chinese Physica B 26(2), 027503 (2017); https://doi.org/10.1088/1674-1056/26/2/027503

[30] J. P. Perdew, K. Burke, and M. Ernzerhof, Physical review letters 77(18), 3865 (1996); https://doi.org/10.1103/PhysRevLett.77.3865

[31] L. M. Malard, K. F. Mak, A. C. Neto, N. M. R. Peres, and T. F. Heinz. New Journal of Physics 15(1), 015009 (2013); https://doi.org/10.1088/1367-2630/15/1/015009

[32] S. A. Abbas, M. Rashid, M. A. Faridi, M. B. Saddique, A. Mahmood, and S. M. Ramay, Journal of Physics and Chemistry of Solids 113, 157-163 (2018);https://doi.org/10.1016/j.jpcs.2017.10.020

[33] Z. Souadia, A. Bouhemadou, S. Bin-Omran, R. Khenata, Y. Al-Douri, and S. Al Essa, Journal of Molecular Graphics and Modelling 90, 77-86 (2019);https://doi.org/10.1016/j.jmgm.2019.04.008

[34] H. J. Goldsmid, and R. W. Douglas, British Journal of Applied Physics 5(12), 458 (1954); https://doi.org/10.1088/0508-3443/5/11/303

[35] T. M. Tritt, Annual review of materials research 41, 433-448 (2011);https://doi.org/10.1146/annurev-matsci-062910-100453

[36] P. Ruleova, C. Drasar, P. Lostak, C-P. Li, S. Ballikaya, and C. Uher. Materials Chemistry and Physics 119, 299-302 (2010); https://doi.org/10.1016/j.matchemphys.2009.08.067

[37] X. Qu, W. Wang, W. Liu, Z. Yang, X. Duan, D. Jia, Antioxidation, Mater. Chem. Phys. 129, 331 (2011); https://doi.org/10.1016/j.matchemphys.2011.04.022

[38] N. Mansourian-Hadavi, S. Wansom, N. H. Perry, A. R. Nagaraja, T. O. Mason, L. H. Ye, and A. J. Freeman, Physical Review B 81(7), 075112 (2010);https://doi.org/10.1103/PhysRevB.81.075112

[39] R. Ullah, M. A. Ali, G. Murtaza, A. Khan, and A. Mahmood, International Journal of Energy Research 44(11), 9035-9049 (2020); https://doi.org/10.1002/er.5613

[40] T. Ramachandran, N. E. Rajeevan and P.P. Pradyumnan, Materials Sciences and Applications 4(12), 816 (2013); https://doi.org/10.4236/msa.2013.412104

[41] S. F. Rubab, S. Naseem, S. M. Alay-e-Abbas, M. Zulfiqar, Y. Zhao, and S. Nazir, Physical Chemistry Chemical Physics 23(35), 19472-19481 (2021); https://doi.org/10.1039/D1CP03247J